

PACS numbers: 42.65.Ky; 42.70.Mp; 42.70.Qs
DOI: 10.1070/QE2004v034n10ABEH002849

Calculation of SHG in periodically poled crystals by specifying a spatially periodic dependence of the quadratic nonlinearity in a single-domain crystal

V.G. Dmitriev, R. Singh

Abstract. **A method is developed for calculating SHG in linearly homogeneous periodically poled nonlinear crystals (PPNC) by specifying a spatially inhomogeneous periodic distribution of the quadratic-nonlinearity parameter in the form of a 'small-scale' elliptic sine, whose half-period forms one domain with the characteristic 'microplateau' of the nonlinearity parameter and interdomain walls. It is found that, because the domain length should be equal to the coherence length when the quasi-phase-matching condition is fulfilled, and if the coherence length is calculated in the fixed-field approximation, the dependence of the harmonic amplitude on the longitudinal coordinate has the form of a 'large-scale' elliptic sine with a broad 'macroplateau' corresponding to a certain (in the case of quasi-phase matching, to virtually 100 %) transformation; however, the mismatch in a domain is never completely compensated by the reciprocal lattice vector. In this case, the phase trajectories inside one domain have the form of a sequence: an unstable focus, a limit cycle ('macroplateau'), a stable focus. This picture repeats in the next domain. It is shown that the width of the SHG phase-matching curve in a PPNC in the regime of strong energy exchange, taking secondary maxima into account, can be considerably (by several times) larger than the width calculated in the fixed-field approximation.**

Keywords: *harmonic generation, PPNC, quasi-phase matching*.

1. Introduction

Periodically poled nonlinear crystals (PPNCs) are of great interest for application in nonlinear-optical laser radiation frequency converters [1, 2]. The phase matching of the waves of fundamental laser radiation and second harmonic in PPNCs is achieved due to a periodic change in the sign of the quadratic nonlinearity or, which is the same, due to a periodic change in the generalised phase by π. In this case, the coherence length (for a given mismatch) and the domain length should be equal, which corresponds to the so-called quasi-phase-matching condition, when the nonlinear deviation of the generalised phase from its optimal value is periodically compensated by the phase jump by π in passing from one domain to another [2].

The principle of quasi-phase-matching in a periodically nonlinear crystal, which was proposed even at the dawn of nonlinear optics (in 1962) by Bloembergen and co-workers [3] and technologically realised only during the last two decades in PPNCs, attracts great practical interest of researchers and engineers due to a number of interesting and unique properties of such crystals (see details in [2]).

The theory of laser frequency conversion in PPNCs is still far from its completion even concerning SHG, not to mention optical parametric oscillation or generation of difference and sum frequencies. Many aspects of this theory are not developed at all (this concerns first of all the theory of influence of factors limiting the frequency conversion efficiency; these questions were partially discussed in [4] (see also references in [1, 2]). The absence of a complete theory of frequency conversion in such crystals is explained first of all by considerable mathematical difficulties of calculations compared to the theory of frequency conversion in mono-domain (homogeneous) crystals.

The methods for calculating the frequency conversion process in PPNCs can be conditionally divided into the following groups:

(i) The successive calculation of the conversion process from domain to domain, when the output values of amplitudes and phases of the waves of the previous $(n-1)$th domain are the boundary (input) values for the next nth domain. The same also concerns, of course, the space – time distributions of amplitudes and phases in calculations of wave packets [pulses and beams (see, for example, [5])];

(ii) the calculation of the conversion process in a linearly homogeneous crystal by specifying a spatially inhomogeneous (periodic) distribution of the parameter of quadratic nonlinearity (see, for example, [1]);

(iii) the calculation of the conversion process in a linearly homogeneous crystal using the corresponding change of variables by transforming the difference equations for a PPNC to the differential equations for a homogeneous crystal [2, 6].

Because all these calculation methods can give analytic solutions only in simplest cases (plane waves, fixed-field approximation for a strong wave), the results are mainly obtained by computer simulations.

In this paper, we will use the second calculation method by specifying a certain periodic distribution of the quadratic

V.G. Dmitriev M.F. Stel'makh Polyus Research & Development Institute, ul. Vvedenskogo 3, 117342 Moscow, Russia;
R. Singh Department of Physics and Mathematics and Natural Sciences, Peoples' Friendship University of Russia, ul. Miklukho-Maklaya 6, 117198 Moscow, Russia

Received 9 August 2004
Kvantovaya Elektronika **34** (10) 933 – 940 (2004)
Translated by M.N. Sapozhnikov

nonlinearity $\chi^{(2)}(z)$, and make an attempt to take into account interdomain walls in this distribution. We perform calculations by the example of SHG in the plane-wave approximation using truncated equations for a homogeneous crystal. It is obvious that the specific shape of the function $\chi^{(2)}(z)$ is quite important. This function is usually represented in the form of a meander, i.e., a function with the amplitude $\chi_0^{(2)}$, which is constant over the domain length and periodically changes its sign in passing from one domain to another [1]. At the same time, the correctness of such a form of the function $\chi^{(2)}(z)$ is in doubt [7, 8]. Thus, the authors of [7] proved experimentally the existence of interdomain walls of thickness ~ 1 μm (for the domain thickness 5–20 μm), where the spatial dependence of $\chi^{(2)}$ and the behaviour of the optical axis of a crystal are not specified generally speaking. In [8], an interesting attempt was made to analyse a real shape of the function $\chi^{(2)}(z)$ in a PPNC using parametric luminescence and it was assumed that $\chi^{(2)}$ changes linearly inside the interdomain wall from its maximum value $\chi_0^{(2)}$ in the $(n-1)$th domain to the value $-\chi_0^{(2)}$ in the nth domain, while in the next interdomain wall the value of $-\chi_0^{(2)}$ changes from $-\chi_0^{(2)}$ to $\chi_0^{(2)}$. Note also that the refractive index and the absorption coefficient inside the interdomain wall can differ from those inside the domain [7, 9, 10].

2. Theory of SHG in a PPNC formed by a spatially periodic distribution of the parameter $\chi^{(2)}$ taking interdomain walls into account

Formulation of the problem and basic equations. Consider the propagation of laser radiation in a homogeneous (over the refractive index) quadratically nonlinear crystal, in which the nonlinearity parameter $\chi^{(2)}$ is a periodic function of the longitudinal coordinate z. To take the interdomain walls into account, we will assume that this distribution is described by the elliptic sine

$$\chi^{(2)} = \chi_0^{(2)} \mathrm{sn}(u;\kappa), \tag{1}$$

where $\mathrm{sn}(u;\kappa)$ is the two-parameter Jacobi sine [11], which is the solution of the equation

$$\left[\frac{\mathrm{d}\,\mathrm{sn}(u;\kappa)}{\mathrm{d}u}\right]^2 = \left[1-\mathrm{sn}^2(u;\kappa)\right]\left[1-\kappa^2\mathrm{sn}^2(u;\kappa)\right], \tag{2}$$

where $u=\gamma z$; γ is a proportionality coefficient.

The elliptic Jacobi sine $\mathrm{sn}(u;\kappa)$ is a periodic function of the parameter u with a period equal to $4K$, where

$$K(\kappa) = \int_0^1 \left[\left(1-y^2\right)\left(1-\kappa^2y^2\right)\right]^{-1/2}\mathrm{d}y \tag{3}$$

is the complete elliptic integral of the first kind [11, 12]. It follows from (3) that the period of elliptic sine is uniquely determined by the parameter κ. For $\kappa=0$, the elliptic Jacobi sine transforms to usual (trigonometric circular) sine, and for $\kappa=1$ to hyperbolic tangent:

$$\mathrm{sn}(u;0)=\sin u, \quad \mathrm{sn}(u;1)=\tanh u. \tag{4}$$

Correspondingly, for $\kappa=0$, we have $K=\pi/2$ (the total period of sine is $4K=2\pi$) and for $\kappa\to 1$, we obtain $K\to\infty$. Note also that

$$\mathrm{sn}(u;2mK)=0, \quad \mathrm{sn}[u;(4m+1)K]=1,$$

where $m=0,\pm1,\pm2,\ldots$.

By specifying the quadratic nonlinearity in the form of a spatially periodic function, we form in this way a periodically nonlinear crystal, which is homogeneous in a linear approximation (i.e., over the refractive index) but inhomogeneous over its quadratic nonlinearity. We do not consider here the method of synthesis of such an inhomogeneous nonlinear crystal (see, for example, [9]). The description of this periodic inhomogeneity of nonlinearity by the Jacobi sine allows one to realise a structure containing a plateau of the parameter $\chi^{(2)}$ and some region, which can be conditionally called an interdomain wall between adjacent domains, i.e., between the adjacent half-periods of the Jacobi function, in which the signs of the parameter are different (Fig. 1). The absolute value of the parameter $\chi^{(2)}$ decreases inside the wall, passing through zero at points $u/K=0,2,4,\ldots$. Therefore, the periodic structure of nonlinearity forms a peculiar 'domain' structure with the domain length $L_\mathrm{d}=2K/\gamma$, which is constant over the crystal length, and also interdomain walls. In other words, in our case, we form a PPNC.

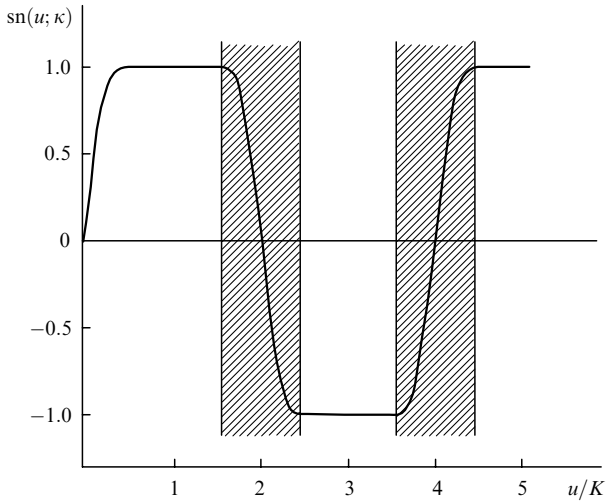

Figure 1. Formation of a PPNC by describing a periodic quadratic nonlinearity by elliptic sine. The interdomain walls are hatched. The domain length is $L_\mathrm{d}=2K/\gamma$.

The question arises of how the periodic structure of quadratic nonlinearity can be correctly taken into account in the calculations of frequency conversion in such periodically nonlinear crystals. Traditionally, these processes are described by using the wave equation [2]

$$\mathrm{rot}\,\mathrm{rot}\,\boldsymbol{E}+\frac{1}{c^2}\frac{\partial^2\boldsymbol{E}}{\partial t^2}=-\frac{4\pi}{c^2}\frac{\partial^2\boldsymbol{P}}{\partial t^2}, \tag{5}$$

where

$$\boldsymbol{P}=\chi^{(1)}\boldsymbol{E}+\chi^{(2)}\boldsymbol{E}^2+\ldots \tag{6}$$

is the polarisability of a dielectric; $\chi^{(1)}=(\varepsilon_0-1)/(4\pi)$ is the

linear susceptibility; $\varepsilon_0 = n^2$ is the linear permittivity; n is the refractive index; $\chi^{(2)}$ is the quadratic susceptibility defined by (1). Because the right-hand side of (5) contains only the time derivative, we can simply substitute (1) into (6) and to include the linear component of polarisability (6) into the left-hand side of (5).

One can easily see that a nonlinear medium under study, which is periodically inhomogeneous over $\chi^{(2)}$, is simultaneously homogeneous over the refractive index n, both in the linear and the next (quadratically nonlinear) approximation. This is due to the fact that the addition Δn to the refractive index in a quadratically nonlinear medium is zero on average over the light oscillation cycle ($\Delta n = n_1 E$, where $n_1 = \chi^{(2)}/2n_o$, and n_o is the linear component of the refractive index.) The inhomogeneity over n can be revealed only in the next, cubically nonlinear approximation ($\Delta n = n_2 E^2$, where $n_2 = \chi^{(3)}/2n_o$), in which the value of Δn averaged over the light-oscillation cycle is no longer zero. We restrict ourselves here to a quadratically nonlinear medium only and neglect weak variations in the refractive index caused by cubic nonlinearity and also neglect variations observed, in particular, experimentally [7].

By neglecting also anisotropy and considering the propagation of laser radiation and the second harmonic along the z axis in a uniaxial crystal in the form of plane waves, we can rewrite (5), together with (6), in the form

$$-\Delta \boldsymbol{E} + \frac{\varepsilon_0}{c^2}\frac{\partial^2 \boldsymbol{E}}{\partial t^2} = -\frac{4\pi}{c^2}\mathrm{sn}(u;\kappa)\chi_0^{(2)}\frac{\partial^2 \boldsymbol{E}^2}{\partial t^2}. \tag{7}$$

By deriving truncated equations in a usual way [2], we obtain, for example, for SHG and interactions of the ooe, eeo, ooo, and eee types (fundamental radiation waves are polarised equally)* the system of equations

$$\begin{aligned}
\frac{\mathrm{d}a_1}{\mathrm{d}z} &= -\sigma_1 \mathrm{sn}(\gamma z;\kappa) a_1 a_2 \sin\psi,\\
\frac{\mathrm{d}a_2}{\mathrm{d}z} &= \sigma_2 \mathrm{sn}(\gamma z;\kappa) a_1^2 \sin\psi,\\
\frac{\mathrm{d}\psi}{\mathrm{d}z} &= \Delta k + \left(\sigma_2\frac{a_1^2}{a_2} - 2\sigma_1 a_2\right)\mathrm{sn}(\gamma z;\kappa)\cos\psi,
\end{aligned} \tag{8}$$

where $a_{1,2}$ are the real amplitudes of laser-radiation and second-harmonic waves, respectively; $\Delta k = k_2 - 2k_1$ is the wave mismatch; $\psi = \Delta k z + 2\varphi_1 - \varphi_2$ is the generalised phase of the process; $\varphi_{1,2}$ are the partial phases of the waves; and $\sigma_{1,2}$ are nonlinear coupling coefficients [2] (they contain now only the nonlinearity amplitude, i.e., $\chi_0^{(2)}$).

One can see from Eqs (8) that, despite the presence of a spatially periodic factor (elliptic sine) in the right-hand side, the first two equations of system (8) have the same first integral as similar equations for conventional SHG in a homogeneous (monodomain) crystal (this integral corresponds to the fulfilment of the Manly–Roy relations):

$$\sigma_2 a_1^2(z) + \sigma_1 a_2^2(z) \equiv \sigma_2 a_1^2(0) + \sigma_1 a_2^2(0) = \sigma_2 a_0^2, \tag{9}$$

*Recall [2] that all the six types of phase-matching are possible in uniaxial PPNCs. For the two remaining types of interaction (eoe and oeo), in which two fundamental waves have orthogonal polarisations, equations for the sum frequency generation should be used [2, 13]. This does not restrict the generality of equations (8).

where the value of a_0 is determined by the boundary values of the wave amplitudes (for $z = 0$). By using (9), we rewrite system (8) in the form

$$\begin{aligned}
\frac{\mathrm{d}a}{\mathrm{d}z} &= \mathrm{sn}(\gamma z;\kappa)(\sigma_2 a_0^2 - \sigma_1 a_2^2)\sin\psi,\\
\frac{\mathrm{d}\psi}{\mathrm{d}z} &= \Delta k + \frac{\sigma_2 a_0^2 - 3\sigma_1 a_2^2}{a_2}\cos\psi\,\mathrm{sn}(\gamma z;\kappa).
\end{aligned} \tag{10}$$

Finally, by introducing the dimensionless variables

$$\upsilon = \left(\frac{\sigma_1}{\sigma_2}\right)^{1/2}\frac{a_2}{a_0},\quad \xi = (\sigma_1\sigma_2)^{1/2} a_0 z,\quad \Delta = \frac{\Delta k}{2(\sigma_1\sigma_2)^{1/2} a_0},$$

$$\alpha = \frac{\gamma}{(\sigma_1\sigma_2)^{1/2} a_0}, \tag{11}$$

we obtain from (10)

$$\begin{aligned}
\frac{\mathrm{d}\upsilon}{\mathrm{d}\xi} &= \mathrm{sn}(\alpha\xi;\kappa)(1-\upsilon^2)\sin\psi,\\
\frac{\mathrm{d}\psi}{\mathrm{d}\xi} &= 2\Delta + \frac{1-3\upsilon^2}{\upsilon}\mathrm{sn}(\alpha\xi;\kappa)\cos\psi.
\end{aligned} \tag{12}$$

We will solve the system of equations (12) with the boundary conditions $\upsilon(0) = 0$, $\psi(0) = \pi/2$ [2].

Quasi-phase matching. For $L_d = l_{coh}$ (where $l_{coh} = \pi/\Delta k$ is the coherence interaction length in the fixed-field approximation of laser radiation [2]), i.e., for $\pi\gamma/\Delta k = 2K$, a peculiar 'spatial resonance' appears, which is called quasi-phase matching in the theory of PPNCs [2]. The wave mismatch Δk in this regime is compensated by the reciprocal lattice vector of the nonlinear susceptibility $\chi^{(2)}$, i.e., the equalities

$$\Delta k = \frac{\pi\gamma}{2K(\kappa)}, \tag{13}$$

$$\Delta = \frac{\pi\alpha}{4K(\kappa)} \tag{14}$$

are satisfied.

Approximation of the elliptic sine of quadratic nonlinearity. To increase the calculation rate in computer simulations of Eqns (12) using Mathcad packets, we employed instead of elliptic sine $\mathrm{sn}(u;\kappa)$ its approximation by the sum [11]

$$\mathrm{sn}(u;\kappa) = \frac{2\pi}{\kappa K(\kappa)}\sum_{n=1}^{p}\left\{\exp\left[-\frac{\pi M(n-1/2)}{K(\kappa)}\right]\times\frac{\sin\left\{(2n-1)\pi u/[2K(\kappa)]\right\}}{1-\exp\left[-\pi M(2n-1)/K(\kappa)\right]}\right\}, \tag{15}$$

where p is the number of approximation terms and $M = K(\sqrt{1-\kappa^2})$.

The curves in Fig. 2 show that, when the parameter κ is close to unity ($\kappa = 1 - 10^{-9}$), in fact in the region $0.99 < \kappa < 1$, expression (15) well approximates $\mathrm{sn}(u;\kappa)$ already for $p > 5$.

Order of calculations. First of all, it is necessary to find the parameter γ. For this purpose, we can use the fact that

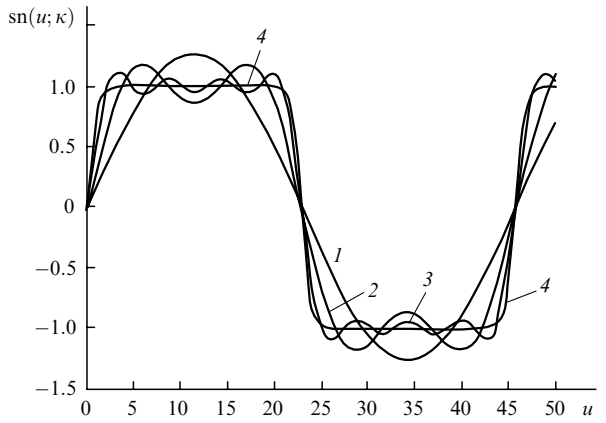

Figure 2. Approximation of elliptic sine by expression (15) for $\kappa = 1 - 10^{-9}$, $K = 11.401$ for $p = 1$ (*1*), 2 (*2*), 5 (*3*), and 10 (*4*).

the dimensionless thickness of the interdomain wall u_w along the coordinate u for the region $0.99 < \kappa < 1$ is always approximately 4. This, in turn, follows from the fact that elliptic sine $\mathrm{sn}(u;\kappa)$ can be replaced by $\mathrm{sn}(u;1)$, i.e., by $\tanh u$ in the region of values of κ, where $\chi^{(2)}$ increases from zero to its maximum. The tabulated values of $\tanh u$ show that this function comes to a plateau at $u \simeq 2$ [12]. Therefore, $u_w = \gamma l_w = 4$ (see Fig. 1), which gives $\gamma = 4/l_w$, where l_w is the interdomain wall thickness. Because the plateau width should be much greater than the interdomain width, the half-period of the function $\mathrm{sn}(u;\kappa)$, i.e., the values of $2K$ should satisfy the condition $2K \gg 4$ or $K \gg 2$. This means that the parameter κ should be close to unity [11, 12]. For example, for $l_w = 1$ μm and $\kappa = 1 - 10^{-9}$, we obtain $\gamma = 4 \times 10^4$ cm^{-1}.

Then, we should determine the parameter $\beta = (\sigma_1\sigma_2)^{1/2}a_0$. Recall that for $a_2(0) = 0$ and $a_1(0) = a_{10}$, we have $a_0 = a_{10}$, where a_{10} is the input ($z = 0$) amplitude of the fundamental (laser) wave. The value of a_{10} (in V cm^{-1}) can be calculated from the expression [2]

$$a_{10} = \left(\frac{752}{n} S_{10}\right)^{1/2},$$

where S_{10} is the laser power density at the crystal input (in W cm^{-2}); n is the refractive index at the laser wavelength. The expression for nonlinear coupling coefficients $\sigma_{1,2}$ contains the parameter d_{eff} – the so-called effective nonlinearity [2] proportional to the amplitude $\chi_0^{(2)}$ (we assume that all the components of the third-rank tensor χ_{ijk} have the same spatiotemporal dependence described by elliptic sine). For example, for $\sigma_{1,2} \approx 2 \times 10^{-5}$ V^{-1} and $a_{10} \approx 2 \times 10^5$ V cm^{-1}, we have $\beta = 4$ cm^{-1}. The value of the parameter β, depending on a particular crystal and laser power density, lies typically in the range from 0.5 to 5 cm^{-1}.

The nonlinear coupling parameters $\sigma_{1,2}$ can be calculated from the expression

$$\sigma_{1,2} = \frac{8\pi^2}{\lambda_1 n_{1,2}} d_{\mathrm{eff}}, \tag{16}$$

where λ_1 is the fundamental radiation wavelength. Let us also present the expression for calculations of d_{eff} for the two most popular PPNCs.

For a lithium niobate crystal ($LiNbO_3$, the $3m$ symmetry group), we have

$$d_{\mathrm{eee}} = (2d_{15} + d_{31})\cos^2\theta\sin\theta + d_{33}\sin^3\theta + d_{22}\cos^3\theta\sin 3\varphi, \tag{17}$$

$$d_{\mathrm{ooo}} = -d_{22}\cos 3\varphi, \tag{18}$$

$$d_{\mathrm{eeo}} = d_{22}\cos^2\theta\cos 3\varphi, \tag{19}$$

$$d_{\mathrm{oeo}} = d_{15}\sin\theta - d_{22}\cos\theta\sin 3\varphi, \tag{20}$$

$$d_{\mathrm{eoo}} = d_{31}\sin\theta - d_{22}\cos\theta\sin 3\varphi, \tag{21}$$

$$d_{\mathrm{oee}} = d_{\mathrm{eoe}} = d_{22}\cos^2\theta\cos 3\varphi, \tag{22}$$

$$d_{\mathrm{ooe}} = d_{15}\sin\theta - d_{22}\cos\theta\sin 3\varphi, \tag{23}$$

and for a potassium titanyl-phosphate crystal (KTP, the $mm2$ symmetry group), we have

$$d_{\mathrm{sss}} = \cos\delta\sin\theta\{-[(2d_{24} + d_{32})\cos^2\varphi + (2d_{15} + d_{31})\sin^2\varphi]\sin^2\delta - \{d_{33}\sin^2\theta + [(2d_{15} + d_{31})\cos^2\varphi + (2d_{24} + d_{32})\sin^2\varphi]\cos^2\theta\}\cos^2\delta + (2d_{15} - 2d_{24} + d_{31} - d_{32})\cos\delta\cos\theta\sin\delta\sin 2\varphi\}, \tag{24}$$

$$d_{\mathrm{fff}} = \sin\delta\sin\theta[-d_{33}\sin^2\delta\sin^2\theta - 2d_{15}(\cos\theta\cos\varphi\sin\delta + \cos\delta\sin\varphi)^2 - d_{31}(\cos\theta\cos\varphi\sin\delta + \cos\delta\sin\varphi)^2 - 2d_{24}(\cos\delta\cos\varphi - \cos\theta\sin\delta\sin\varphi)^2 - d_{32}(\cos\delta\cos\varphi - \cos\theta\sin\delta\sin\varphi)^2], \tag{25}$$

$$d_{\mathrm{ffs}} = \sin\theta\{\cos\delta\{-[d_{24} + (d_{32} - d_{31}\cos^2\theta)\sin^2\delta]\cos^2\varphi - d_{33}\sin^2\delta\sin^2\theta - [d_{15} + (d_{31} - d_{32}\cos^2\theta) \times \sin^2\delta]\sin^2\varphi\} + \tfrac{1}{2}[-d_{15} + d_{24}(d_{31} - d_{32})\cos 2\delta] \times \cos\theta\sin\delta\sin 2\varphi\}, \tag{26}$$

$$d_{\mathrm{sfs}} = \sin\theta\{-[d_{24} + (d_{32} - d_{31}\cos^2\theta)\cos^2\delta]\cos^2\varphi\sin\delta + \cos\delta[d_{15} - d_{24} + (d_{31} - d_{32})\cos 2\delta]\cos\theta\cos\varphi\sin\varphi - \sin\delta\{d_{15}\sin^2\varphi + [d_{33}\sin^2\theta + (d_{31} - d_{32}\cos^2\theta)\sin^2\varphi]\cos^2\delta\}. \tag{27}$$

The components d_{ij} of the tensor entering the expressions for d_{eff} are presented in handbook [13]. The expression for d_{eff} in biaxial crystals contains the additional angle δ

Table 1.

Crystal	Crystal type	Interaction type	$\Delta k/\mathrm{cm}^{-1}$	$l_{\mathrm{coh}}/\mu\mathrm{m}$
KDP	Uniaxial	ooe	−2960.65	10.6
	($\theta = 90^\circ$)	ooo	2371.27	13.2
		eee	1442.39	21.8
		oeo	4572.79	6.9
		eeo	6774.30	4.6
		eoe	−759.13	41.4
$LiNbO_3$	Uniaxial	ooe	1175.89	26.7
	($\theta = 90^\circ$)	ooo	13117.41	2.4
		eee	11157.78	2.8
		oeo	18108.36	1.7
		eeo	23099.30	1.4
		eoe	6166.83	5.1
$LiIO_3$	Uniaxial	ooe	−13076.40	2.4
	($\theta = 90^\circ$)	ooo	5897.94	5.3
		eee	4563.51	6.9
		oeo	14717.89	2.1
		eeo	23537.85	1.3
		eoe	−4256.44	7.4
BBO	Uniaxial	ooe	1605.80	19.6
	($\theta = 90^\circ$)	ooo	2716.47	11.6
		eee	1943.85	16.2
		oeo	14717.89	10.9
		eeo	2885.49	10.3
		eoe	1774.83	17.7
KTP	Biaxial	ssf ($\varphi = 0$)	−4294.30	7.3
	($\theta = 90^\circ$)	ssf ($\varphi = 90^\circ$)	−5755.82	5.5
		ffs ($\varphi = 0$)	18628.59	1.7
		ffs ($\varphi = 90^\circ$)	19663.83	1.6
		sff ($\varphi = 0$)	865.82	36.3
		sff ($\varphi = 90^\circ$)	−78.08	402.3
		sfs ($\varphi = 0$)	13468.48	2.3
		sfs ($\varphi = 90^\circ$)	13986.10	2.2
		sss ($\varphi = 0$)	8308.36	3.8
		sss ($\varphi = 90^\circ$)	8308.36	3.8
		fff ($\varphi = 0$)	6025.93	5.2
		fff ($\varphi = 90^\circ$)	5599.65	5.6
LBO	Biaxial	ssf ($\varphi = 0$)	268.05	117.2
	($\theta = 90^\circ$)	ssf ($\varphi = 90^\circ$)	−3283.75	9.6
		ffs ($\varphi = 0$)	4044.75	7.8
		ffs ($\varphi = 90^\circ$)	7298.09	4.3
		sff ($\varphi = 0$)	1205.31	26.1
		sff ($\varphi = 90^\circ$)	−719.83	43.6
		sfs ($\varphi = 0$)	3107.49	10.1
		sfs ($\varphi = 90^\circ$)	4734.16	6.6
		sss ($\varphi = 0$)	2170.23	14.5
		sss ($\varphi = 90^\circ$)	2170.23	14.5
		fff ($\varphi = 0$)	2142.57	14.7
		fff ($\varphi = 90^\circ$)	1844.10	17.0
$KNbO_3$	Biaxial	ssf ($\varphi = 0$)	27689.61	1.1
	($\theta = 90^\circ$)	ssf ($\varphi = 90^\circ$)	35701.21	0.9
		ffs ($\varphi = 0$)	−515.55	60.9
		ffs ($\varphi = 90^\circ$)	−5397.92	5.8
		sff ($\varphi = 0$)	21346.23	1.5
		sff ($\varphi = 90^\circ$)	26916.65	1.2
		sfs ($\varphi = 0$)	5827.83	5.4
		sfs ($\varphi = 90^\circ$)	5386.65	9.3
		sss ($\varphi = 0$)	12171.21	2.6
		sss ($\varphi = 90^\circ$)	12171.21	2.6
		fff ($\varphi = 0$)	15002.86	2.1
		fff ($\varphi = 90^\circ$)	18132.09	1.7

[along with the polar (θ) and azimuthal (φ) angles], which is described by the expression [2]

$$\cot 2\delta = \frac{\cot^2\Omega\sin^2\theta + \sin^2\varphi - \cos^2\theta\cos^2\varphi}{\cos\theta\sin 2\varphi}, \qquad (28)$$

where the angle Ω specifies the tilt angle of optical axes with respect to the Z axis of the crystal:

$$\cot^2\Omega = \frac{n_x^2}{n_z^2}\frac{n_y^2 - n_z^2}{n_x^2 - n_y^2}; \qquad (29)$$

where n_x, n_y, n_z are the principal values of the refractive index of the crystal. The complete algorithm for calculating the effective nonlinearity parameter d_{eff} in biaxial crystals is described in [2].

The next step is the determination of the coherence interaction length l_{coh} for the specified mismatch Δk. As mentioned above, it was calculated in the fixed-field approximation. Table 1 presents the values of l_{coh} calculated for seven types of nonlinear crystals for $\lambda_1 = 1.064$ μm, $\theta = 90^\circ$ (the XY plane of the crystal) and all the six possible types of phase matching, the calculation for biaxial crystals being performed for two angles φ (0 and 90°), i.e., in the principal planes of the crystal. We used in calculations the values of the refractive indices from handbook [13].

One can see from Table 1 that Δk can vary within a broad range, from 78 cm^{-1} (KTP, sff phase matching for $\varphi = 90^\circ$) up to 3.6×10^4 cm^{-1} ($KNbO_3$, ssf phase matching for $\varphi = 90^\circ$), the coherence length changing from 400 to 0.9 μm. At the same time, the typical values of Δk lie in the range from 1000 to 5000 cm^{-1}, and those of the coherence length in the range from 30 to 6 μm.

Knowing the parameters γ, β, and Δk, we determine using Eqn (13) the complete elliptic integral of the first kind $K = \pi\gamma/(2\Delta k)$. Instead of $\mathrm{sn}(\alpha\xi;\kappa)$ in the right-hand sides of (12), we substitute the approximating function (15), where $u = \alpha\xi$. Note that in the range of κ values close to unity (this range, which corresponds to real PPNCs, is used for calculations), we can reliably set $\kappa = 1$ and $K = M(\sqrt{1-\kappa^2}) = \pi/2$ in expression (15) [11, 12]. The value of α is determined from the expression $\alpha = \gamma\beta^{-1}$. Thus, we completely determine the function $\mathrm{sn}(\alpha\xi;\kappa)$ entering the right-hand sides of Eqns (12) and can start to solve these equations.

Calculation results. Figure 3 shows the dependences of the normalised (dimensionless) amplitude of the second harmonic on the normalised coordinate for different parameters $l_{\mathrm{coh}} = \pi/\Delta k$ for few domains, i.e., the half-periods of the function $\mathrm{sn}(\alpha\xi;\kappa)$, near the input surface of the crystal ($\xi = 0$). We used the following parameters in the calculations: $K = 20$, $\sigma_{1,2} = 2 \times 10^{-5}$ V^{-1}, $a_{10} = 2 \times 10^5$ V cm^{-1}, $\Delta k = 1500$ cm^{-1}, $\beta = 4$ cm^{-1}, $\alpha = 4.775 \times 10^3$, $\gamma = 1.91 \times 10^4$ cm^{-1}, $L_{\mathrm{d}} = 2K/\gamma = 20.94$ μm, $l_{\mathrm{w}} = 2.1$ μm, and $p = 30$.

For curve (*1*) (Fig. 3), the phase-matching condition $l_{\mathrm{coh}} = L_{\mathrm{d}}$ is fulfilled, which corresponds to the dimensionless mismatch $\Delta = 187.5$ [linear increase of $v(\xi)$]. To curves (*2*), (*3*), and (*4*), the 'non-quasi-phase-matching' values $\Delta = 185.625$, 183.75, and 181.875 correspond, respectively. In these cases, the integral dependence $v(\xi)$ also resembles elliptic sine. To avoid misunderstanding, we will call this elliptic sine $v(\xi)$ the 'large-scale' elliptic sine in contrast to the elliptic sine of quadratic nonlinearity $\chi^{(2)}(z)$, which we

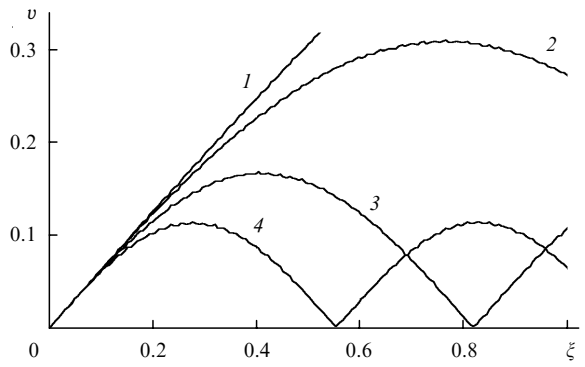

Figure 3. Dependences of the normalised second-harmonic amplitude $\upsilon(\xi)$ calculated for a few domains near the input face of a PPNC for the normalised mismatchs $\Delta = 187.5$ (quasi-phase matching) (*1*), 185.625 (*2*), 183.75 (*3*), and 181.875 (*4*).

will call the 'small-scale' sine [thereby emphasising that the dependence $\upsilon(\xi)$ has the characteristic scale of the order of the crystal length, whereas the characteristic scale of the dependence $\chi^{(2)}(z)$ is of the order of the domain length]. The 'large-scale' elliptic sine is the result of a peculiar interference between the actions of the 'small-scale' elliptic sine $\mathrm{sn}(\alpha\xi;\kappa)$ of quadratic nonlinearity and circular sine $\sin\psi$ of the generalised phase in Eqns (12). Curves $\upsilon(\xi)$ are modulated by spatial oscillations corresponding to the beats of the second-harmonic amplitude in the fixed-field approximation inside each of the domains [$\upsilon \sim \sin(\Delta k z/2) = \sin(\xi\Delta)$] [2]. Note also that because the dimensionless amplitude υ is the second-harmonic amplitude normalised to the laser input radiation amplitude, the quantity υ is in fact the amplitude SHG efficiency (correspondingly, the quantity υ^2 is the power density SHG efficiency).

It is obvious that spatial beats corresponding to the dependence $\sin(\xi\Delta)$ inside domains over large lengths at large amplitudes ξ will not be observed on curves $\upsilon(\xi)$. This is confirmed by Fig. 4, where several curves $\upsilon(\xi)$ are shown near quasi-phase-matching conditions (13), (14) satisfied for different mismatchs Δ. Curves $\upsilon(\xi)$ are almost exactly described the 'large-scale' elliptic sine. It is most interesting here that even when the phase-matching condition $l_{\mathrm{coh}} = L_{\mathrm{d}}$ is exactly fulfilled, or, which is the same, when conditions (13) and (14) are fulfilled, the dependence $\upsilon(\xi)$ differs from hyperbolic tangent, as would be the case for conventional

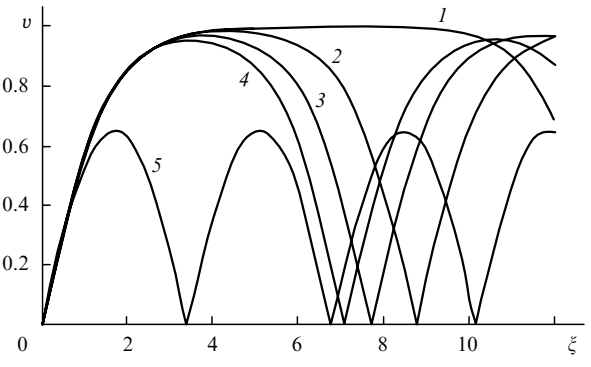

Figure 4. Dependences of the normalised second-harmonic amplitude $\upsilon(\xi)$ calculated for the full length of a PPNC for the normalised mismatch $\Delta = 187.5$ (quasi-phase matching) (*1*) 187.519 (*2*), 187.538 (*3*), 187.556 (*4*), and 188.063 (*5*).

SHG in a homogeneous (single-domain) crystal when the phase-matching condition is exactly fulfilled [2]. In other words, even in the case of quasi-phase matching, the dependence $\upsilon(\xi)$ preserves the form close to the conventional elliptic Jacobi sine [11, 12] with the characteristic plateau. Such behaviour of $\upsilon(\xi)$ implies the presence of a nonzero generalised mismatch, which cannot be compensated by the reciprocal crystal lattice vector whatever the parameters of the process may be. In turn, this is explained by the fact that, as shown in [4, 6] (see also [2]), the coherence interaction length l_{coh} in the next approximation is a function of the second-harmonic wave amplitude:

$$l_{\mathrm{coh}} = \frac{\pi}{\Delta k}\left(1 + \frac{3\upsilon^2 - 2}{2\Delta^2}\right). \tag{30}$$

It follows from (19) that the true coherence length, first, differs from the length $(\pi/\Delta k)$ used in our calculations and, second, changes from $l_{\mathrm{coh}}^{(1)} = (\pi/\Delta k) \times (1 - 1/\Delta^2)$ for the first domains near the input surface of the crystal up to $l_{\mathrm{coh}}^{(2)} = (\pi/\Delta k)[1 + 1/(2\Delta^2)]$ at the point where $\upsilon(\xi)$ achieves the maximum ($\upsilon = 1$). The difference of these values is $3\pi/(2\Delta k\Delta^2)$, which for $\Delta \approx 200$ gives the correction to our coherence length of the order of $3/(2\Delta^2) \approx 4 \times 10^{-5}$. Nevertheless, it is the neglect of this small correction that leads to a periodic mismatch of the generalised phase.

Comments to the phase portrait of the process. One can see from Eqns (12) that the second integral of the system (i.e., the equation of the phase plane [2]) cannot be obtained in the general case of the absence of phase matching in the domain ($\Delta \neq 0$) because the expression for the derivative $\mathrm{d}\psi/\mathrm{d}\upsilon$ will retain the dependence of the longitudinal coordinate ξ. This dependence disappears only for $\Delta = 0$ (the latter fact is of special interest, but its discussion is beyond the scope of this paper). The dependence of the equation for the phase plane on the longitudinal coordinate for $\Delta \neq 0$ means physically the presence of peculiar losses of the second-harmonic energy related to a change in the sign of $\chi^{(2)}(\xi)$ and, hence, of the sign of the derivative $\mathrm{d}\upsilon/\mathrm{d}\xi$. Note that such losses (also periodical) will appear already when the domain length $L_{\mathrm{d}} = 2K/\gamma$ only slightly differs from the coherence interaction length $l_{\mathrm{coh}} = \pi/\Delta k$. In this connection the phase plane should exhibit in the general case not closed curves, as for a conservative system [2], but more complicated, self-crossing in the general case, curves illustrating the above-mentioned peculiar periodic interference of the elliptic [$\mathrm{sn}(\alpha\xi;\kappa)$] and trigonometric [$\sin\psi$ (12)] sines. It is impossible to obtain analytic expressions for such phase trajectories. In separate small parts of the crystal, these trajectories can be curves of the type of stable or unstable focus or unstable limit cycles even when quasi-phase-matching conditions (13) and (14) are fulfilled.

The phase plane of the process corresponding to the fulfilment of the quasi-phase-matching conditions [curve (*1*) in Fig. 3] for several first domains (near the input face of the crystal) is shown in Fig. 5. Unlike SHG in a homogeneous crystal ($\chi^{(2)}(z) \equiv \chi_0^{(2)}$) in the case of exact phase matching ($\Delta k = 0$), when the increase in the harmonic amplitude corresponds to the motion of an imaging point in the υ, ψ phase plane along the separatrix coming from the coordinate origin, with the constant generalised phase $\psi(\xi) \equiv \pi/2$ [2], in this case the motion of an imaging point corresponds to an unstable focus. This is explained by the fact that in the case of an exact fulfilment of the quasi-

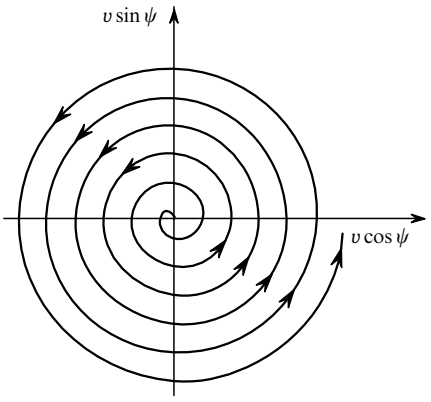

Figure 5. Phase plane of SHG (unstable focus) in a PPNC for quasi-phase-matching conditions satisfied for the first five domains near the input face of the crystal. The phase rotation by 2π corresponds to the propagation of one domain by light.

phase-matching condition, the equality $d\upsilon/d\xi = 0$ (i.e., $\psi = \pi$) is satisfied at the output from each of the domains and the condition $\xi = 2K/\alpha$, i.e., $\mathrm{sn}(\alpha\xi;\kappa) = 0$ is also fulfilled simultaneously. In a PPNC with periodic quadratic nonlinearity in the form of a spatial meander [$\chi^{(2)}(z) = \pm\chi_0^{(2)}$], the phase ψ experiences a jump by π in passing between domains. However, such a jump does not occur in our case, and the phase ψ increases uniformly and linearly with coordinate ξ, turning by 2π during the propagation of the wave inside the domain. The number of turns is equal to the number of domains. It was pointed out in [8] that this model is closer to reality than the model of a PPNC with meander.

Therefore, the phase trajectory of the SHG process in a PPNC with a periodic dependence of $\chi^{(2)}(z)$ in the form of elliptic sine (considering the presence of domain walls) for few domains near the input surface of this crystal forms an unstable focus even when the quasi-phase-matching condition is fulfilled. Later, the phase trajectories come to the limit cycle corresponding to the maximum conversion efficiency 100 % ($\upsilon = 1$) and to a plateau in the 'large-scale' elliptic sine. Detailed calculations showed that, by coming to the limit cycle ($\upsilon = 1$) and 'remaining' in it during the time for which the wave propagates a certain distance in the crystal, the phase trajectories leave the limit cycle by forming a stable focus. However, unlike the behaviour of $\upsilon(\xi)$ in the case of a conventional stable focus [14], here the value of $\upsilon(\xi)$ achieves zero and begins immediately to increase – the unstable focus, limit cycle, and stable focus are repeated again, etc.

Such a form of phase trajectories emphasises once more the oscillatory-wave similarity of nonlinear processes in physics or, in other words, the spatiotemporal analogy between oscillatory processes in systems with lumped constants (for example, in radio circuits) and wave processes in systems with distributed parameters [2, 14]. In our case, the increase in the harmonic amplitude along the coordinate ξ is equivalent to the growth of oscillations and coming to the limit cycle in time for a nonlinear oscillator with saturation and negative losses (i.e., amplification); the gain is characterised in this case by the parameter β. We have failed so far to find a complete radiophysical analogy of a periodically repeated series involving an unstable focus – a limit cycle – a stable focus. We can assume that similar phenomena can be observed in radio-frequency generators with a thermistor in the circuit or feedback loop. The 'transfer' of some characteristic phase trajectories to others, which we observed, is explained by the presence of the principally uncompensated nonzero generalised mismatch Δ_{gen} even under the condition of quasi-phase matching ($l_{\mathrm{coh}} = L_{\mathrm{d}}$). If we take the coherence length not in the fixed-field approximation but in the approximation described by expression (19), the phase-matching conditions will be fulfilled only at an only point on the crystal length, whereas along the rest of the crystal length, SHG will occur with some small but noticeable mismatch depending on the length z.

Therefore, a strictly regular domain structure of the crystal under study (with the constant domain length $L_{\mathrm{d}} = 2K/\gamma$ over the crystal length) is not, generally speaking, optimal for SHG, although the requirement of the presence of hyperbolic tangent in the dependence $\upsilon(\xi)$ seems redundant from the practical point of view. At the same time, we can determine the generalised mismatch Δ_{gen} from curve (*1*) in Fig. 4 corresponding to quasi-phase matching by using the expressions [2]

$$\upsilon_{\max} = (\kappa')^{1/2} = \left[1 + \left(\frac{\Delta_{\mathrm{gen}}}{2}\right)^2\right]^{1/2} - \frac{\Delta_{\mathrm{gen}}}{2}, \tag{31}$$

$$\Delta_{\mathrm{gen}} = \frac{1-\kappa'}{(\kappa')^{1/2}} = \frac{1-\upsilon_{\max}^2}{\upsilon_{\max}}. \tag{32}$$

Therefore, knowing $\upsilon_{\max}$, we can find parameters κ' [corresponding to the integral 'large-scale' elliptic sine $\upsilon(\xi)$] and Δ_{gen}. Thus, for $\upsilon(\xi) = 0.997$, we have $\Delta_{\mathrm{gen}} = 6 \times 10^{-3}$, which is only 3×10^{-3} % of the parameter Δ. Obviously, this correction can be neglected in practice.

Figure 6 shows the phase-matching curve $\upsilon(\Delta)$ for SHG in the PPNC at its constant length [curve (*1*)]. The maximum of the second-harmonic amplitude is achieved in our case for $\Delta = 187.5$, which corresponds to the fulfilment of the quasi-phase-matching condition (see also Fig. 3). Figure 6 also shows the optimised curve $\upsilon_{\max}(\Delta)$, which illustrates the dependence of the maximum amplitude of the second harmonic (which is achieved, generally speak-

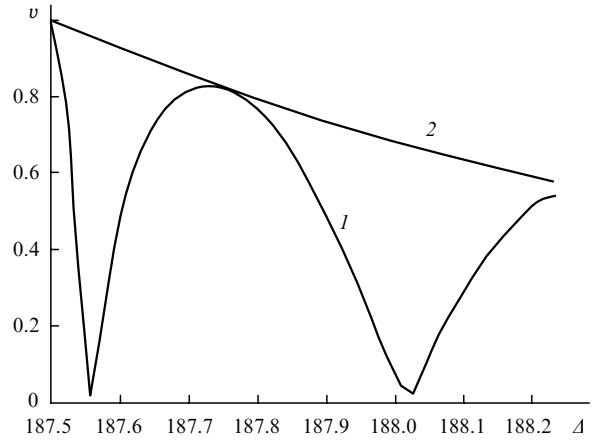

Figure 6. Quasi-phase-matching curve $\upsilon(\Delta)$ for a constant length of the crystal (*1*) and the optimised curve $\upsilon_{\max}(\Delta)$ for different crystal lengths (*2*) in a substantially nonlinear conversion regime ($\beta = 4\ \mathrm{cm}^{-1}$). For $\Delta = 187.5$, quasi-phase matching is realised.

ing, at different lengths ξ) on the parameter Δ [curve (*2*)]. Curve (*1*) has two specific features: its zeroes are non-equidistant (recall that the zeroes of the phase-matching curve are equidistant in the fixed-field approximation [2]) and the amplitudes of secondary maxima are large and comparable with that of the central maximum. These effects are well known for SHG in a strong energy exchange regime (see, for example, our paper [15]). An important practical conclusion following from the consideration of these curves is that the calculation of the phase-matching width in such a regime only from the width of the central maximum, as accepted in the fixed-field approximation, will lead to a considerable error. It is necessary to consider secondary maxima (second and even probably the third one). As a result, the width of the phase-matching curve for SHG in a PPNC in the strong energy exchange regime can be substantially (by several times) greater than that calculated in the fixed-field approximation. Because the central maximum of the phase-matching curve is narrow, it may be expedient in some cases to violate quasi-phase matching, by choosing the generalised mismatch corresponding to the centre of the second maximum (in Fig. 6, this corresponds to $\Delta = 187.75$).

3. Conclusions

We have developed the method for calculating the frequency conversion process (by the example of SHG) by specifying a spatially inhomogeneous periodic distribution of the quadratic nonlinearity parameter in the form of elliptic sine, whose half-period forms one domain with the characteristic plateau of the nonlinearity parameter and interdomain walls. We have shown that, when the quasi-phase-matching condition is fulfilled and the half-period of elliptic sine, i.e., the length of one domain, is equal to the coherence length, the dependence of the harmonic amplitude on the longitudinal coordinate has the form of 'large-scale' elliptic sine with a broad plateau corresponding to 100 % conversion; however, the mismatch in the domain cannot be completely compensated by the reciprocal lattice vector whatever parameters may be.

The parameters of 'large-scale' elliptic sine allow one to calculate this principally uncompensated mismatch. The mismatch appears due to the difference of the coherence length, used in calculations in the fixed-field approximation, from the real coherence length (30) depending on the harmonic amplitude and, hence, on the longitudinal coordinate. At the same time, the corresponding correction is negligibly small in practice. The phase trajectory of the SHG process in the case of quasi-phase matching forms an unstable focus, a limit cycle (the harmonic amplitude remains constant at many domains, but the generalised phase inside each of the domains changes by 2π), and a stable focus in each half-period of 'large-scale' elliptic sine. This situation is completely repeated in the second half-period. The width of the phase-matching curve should be calculated taking the secondary maxima into account. As a result, the width of the phase-matching curve for SHG in the strong energy exchange regime can be substantially (by several times) greater than that calculated in the fixed-field approximation. The method for calculating the SHG process in PPNCs developed in the paper, which takes interdomain walls into account, can be efficiently used to calculate the conversion efficiency in diverging laser beams. This method allows one to take into account the anisotropy of the crystal and the effect of thermal self-actions, as well as transient phenomena in various regimes of generation of sum and difference frequencies and optical parametric oscillation.

References

1. Feier M.M., Magel G.A., Jundt D.H., Byer R.L. *IEEE J. Quantum Electron.*, **28**, 2631 (1982); Rustagi K.C., Mehendale S.C., Meenakshi S. *IEEE J. Quantum Electron.*, **18**, 1029 (1982).
2. Dmitriev V.G., Tarasov L.V. *Prikladnaya nelineinaya optika* (Applied Nonlinear Optics) (Moscow: Fizmatlit, 2004).
3. Armstrong J.A., Bloembergen N., Ducuing J., Pershan P.S. *Phys. Rev.*, **127**, 1918 (1962).
4. Yur'ev Yu.V. *Cand. Diss.* (Moscow: MIPT, 2001).
5. Abashin M.V. *Master Sci. Thesis* (Moscow: MIPT, 2003).
6. Dmitriev V.G., Yur'ev Yu.V. *Kvantovaya Elektron.*, **28**, 259 (1999) [*Quantum Electron.*, **29**, 814 (1999)].
7. Aleksandrovskii A.A., Gliko O.A., Naumova I.I., Pryalkin V.I. *Kvantovaya Elektron.*, **23**, 657 (1996) [*Quantum Electron.*, **26**, 641 (1996)].
8. Kitaeva G.Kh., Penin A.N. *Kvantovaya Elektron.*, **34**, 597 (2004) [*Quantum Electron.*, **34**, 597 (2004)]; Kitaeva G.Kh., Penin A.N. *Zh. Eksp. Teor. Fiz.*, **125**, 307 (2004).
9. Miller G.D. *Dissertation for the Degree of Doctor of Philosophy* (Stanford University, USA, 1998).
10. Golenishchev-Kutuzov A.V., Golenishchev-Kutuzov V.A., Kallimulin R.I. *Indutsirovannye domennye struktury v elektro- i magnitouporyadochennykh veshchestvakh* (Induced Domain Structures in Electrically- and Magnetically Ordered Materials) (Moscow: Fizmatlit, 2003).
11. *Higher Transcendental Functions* (Bateman Manuscript Project), Vols. 1–3, ed. by A. Erdelyi (New York: McGraw-Hill, 1955; Moscow: Nauka, 1967).
12. Jahnke E., Emde F., Losch F. *Tables of Higher Functions* (New York: McGraw-Hill, 1960; Moscow: Nauka, 1977).
13. Dmitriev V.G., Gurzadyan G.G., Nikogosyan D.N. *Handbook of Nonlinear Optical Crystals* (New York, Berlin: Springer-Verlag, 1999).
14. Rabinovich M.I., Trubetskov D.I. *Vvedenie v teoriyu kolebanii i voln* (Introduction to the Theory of Oscillations and Waves) (Moscow: Izd. NITs 'Regular and Chaotic Dynamics', 2000).
15. Guk D.A., Dmitriev V.G. *Kvantovaya Elektron.*, **18**, 106 (1991) [*Sov. J. Quantum Electron.*, **21**, 96 (1991)].